ECS Transactions, 35 (1) 2077-2084 (2011)
10.1149/1.3570198 ©The Electrochemical Society

The Structural Disorder and Lattice Stability of (Ba,Sr)(Co,Fe)O_3 Complex Perovskites

M. M. Kuklja[a], Yu. A. Mastrikov[a, b], S. N. Rashkeev[c], and E. A. Kotomin[b, d]

[a] Materials Science and Engineering Department, University of Maryland, MD, USA
[b] Institute for Solid State Physics, University of Latvia, Kengaraga str. 8, Riga, Latvia
[c] Center for Advanced Modeling and Simulations, Idaho National Laboratory, USA
[d] Max Planck Institute for Solid State Research, Heisenbergstr. 1, Stuttgart, Germany

The structural disorder and lattice stability of complex perovskite (Ba,Sr)(Co,Fe)O_3, a promising cathode material for solid oxide fuel cells and oxygen permeation membranes, is explored by means of first principles DFT calculations. It is predicted that Ba and Sr ions easily exchange their lattice positions (A-cation disorder) similarly to Co and Fe ions (B-cation disorder). The cation antisite defects (exchange of A- and B-type cations) have a relatively high formation energy. The BSCF is predicted to exist in an equilibrium mixture of several phases and can decompose exothermically into the Ba- and Co-rich hexagonal (Ba,Sr)CoO_3 and Sr- and Fe-rich cubic (Ba,Sr)FeO_3 perovskites.

Introduction

Novel advanced materials are urgently needed for new sources of ecologically clean energy. The complex $Ba_xSr_{1-x}Co_{1-y}Fe_yO_{3-\delta}$ (BSCF) perovskites are currently considered as promising materials for cathodes in solid oxide fuel cells (SOFC) and oxygen permeation membranes [1,2]. This class of perovskites exhibits a good oxygen exchange performance and mixed ionic and electronic conductivity. The low oxygen vacancy formation energy, characteristic of these perovskites, leads to the high oxygen vacancy concentration, and the relatively low activation barrier for the vacancy diffusion causes the high ionic mobility [3]. Those factors largely define the oxygen reduction chemistry of these materials [4,5].

Understanding and predicting the structure-property-function relationship in BSCF and similar materials is far from being complete. For example, it was suggested that cubic BSCF is less stable than expected and tend to transform into hexagonal phase or even to decompose slowly at temperatures around 1000 K [6,7]. The relationship between the structural disorder in BSCF and its crystalline stability is extraordinarily complex and essentially unexplored.

In this short paper, we present results of first principles calculations of BSCF and related ABO_3 –type perovskites. We simulate both an ideal BSCF crystal and the crystal containing a range of point defects. In addition to Frenkel and Schottky disorders, we analyze rearrangements in cation sublattices, such as antisite defects and substitutions that lead to the clustering effect of either A or B metals. We also analyze a variety of possible solid state chemical reactions that simulate the decomposition of the original

BSCF crystal into other perovskites and binary oxides. We discuss our results in the context of available experimental data.

Details of Periodic *ab initio* Calculations

The results were obtained by means of the DFT method as implemented in the computer code VASP 4.6 [8]. Projector Augmented Wave (PAW) scalar relativistic pseudopotentials were used. The exchange-correlation GGA functional was of PBE-type. In the library of potentials, supplied with the VASP code, there is a single PAW PBE potential for each of Ba, Sr and Co elements and multiple potentials for Fe and O, which differ by the number of valence electrons and the basis set cut-off energy, respectively. Our test calculations showed practically no dependence of the lattice constant (<0.05%) as well as the binding energy (<0.4%) of the BSCF on the choice of Fe PAW PBE potentials. For O, we used soft PAW PBE potential, which gives the binding energy very close the experimental value and a reasonable bond length for a free O_2 molecule (5.24 eV and 1.29 Å, cf. with the experimental values of 5.12 eV and 1.21Å, respectively).

The 8x8x8 k-point mesh was created by the Monkhorst-Pack scheme [9] for the ABO_3 unit cell. Ionic charges were calculated by the Bader method [10]. The kinetic energy cut-off for the plane wave basis set was set to 520 eV.

Defects were simulated using periodic supercells that were constructed by expanding the five-atom primitive unit cell by 2x2x2 (40 atoms) shown in Fig.1 [4] and by 4x4x4 (320 atoms). The effective charges of both Sr and Ba are close to a formal charge of +2e and practically do not change with the chemical composition, whereas the charges on both B-metals are much smaller than their formal charges of +4e. The effective charge on O (-1.15e) is also strongly reduced compared to the formal charge of -2e. This stems from the considerable covalent contribution into the B-O chemical bonding, which is typical for ABO_3 perovskites. A significant degree of covalency, illustrated by the electronic density map in Fig.2, plays an important role in defect energetics discussed below.

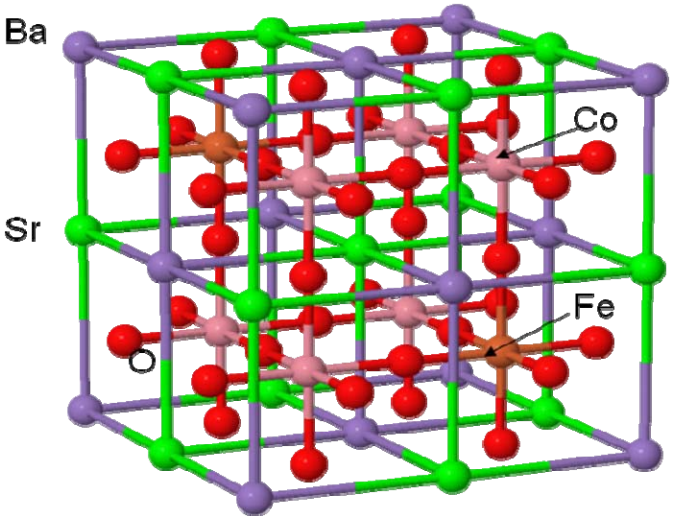

Figure 1. The $Ba_{0.5}Sr_{0.5}Co_{0.75}Fe_{0.25}O_3$ crystal structure is represented by a 40 atom supercell. The red balls denote oxygen atoms.

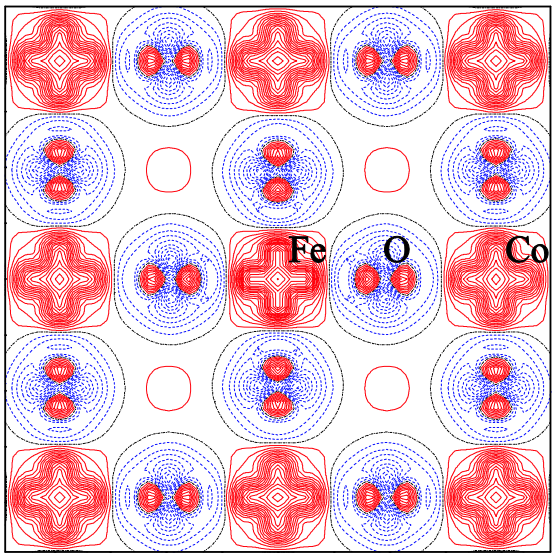

Figure 2. Difference electronic density map of the $Co_{0.75}Fe_{0.25}O_2$ plane is shown with the increment of $0.032e/Å^3$. Solid red and dash blue lines correspond to positive and negative charges, respectively.

The Energies of Disorder and Decomposition Reactions of BSCF Crystals

In addition to Frenkel (Table 1), Schottky, and cation sublattice disorders (Table 2), we studied a large set of possible solid state decomposition reactions for the most efficient $Ba_{0.5}Sr_{0.5}Co_{0.75}Fe_{0.25}O_3$ composition solid solutions (Table 3).

Among Frenkel defects, the oxygen vacancy-interstitial pairs have the lowest formation energy of 1.2-1.46 eV per defect, with some preference given to the oxygen vacancy placed between Co and Fe atoms in the BSCF lattice rather than between two Co atoms (Table 1). The result is in agreement with the formation energies for relevant single oxygen vacancies [5]. This trend remains valid for both the closest and the distant defect pairs. Note that the formation energies for oxygen Frenkel defects in BSCF turn out to be much smaller than in other perovskites, e.g. $SrTiO_3$ (~10 eV [11]) which means that the easier defect formation will lead to the higher concentration of defects.

Energy of Schottky disorder is calculated from equation (1):

$$0 \rightarrow 2V''_{Ba}+2V''_{Sr}+3V'''_{Co}+V''''_{Fe}+12V^{\cdot\cdot}_{O} \qquad (1)$$

Schottky disorder can be interpreted as a process of building the BSCF crystal out of supercells that contain a single vacancy each. Hence, there are no ideal fragments in the crystal but rather all supercells are short of a single atom. Thus, the energy of Schottky disorder is relevant to the crystal binding energy per atom and to the formation energy of single isolated vacancies in the crystal. Equation (1) yields the energy of 6.0 eV per one 40 atom supercell (eight BSCF formula units). This is, indeed, consistent with the cohesive energy of 5.13 eV per atom (or 25.64 eV per one BSCF unit cell) and with the range of formation energies of single vacancies in BSCF (3.96 eV for Oxygen and 8.63-

9.76 eV for cations). The left side of equation (1) corresponds to a minimal supercell consisting of $4Ba_{0.5}Sr_{0.5}Co_{0.75}Fe_{0.25}O_3$ units that allows us to keep an even number of atoms in the model cell, while the reaction energy is normalized per the supercell used in calculations (40 atomic supercell) to make it comparable to other energies analyzed here.

Overall, Frenkel (vacancy-interstitial) disorder is preferred over Schottky (vacancy) disorder in the otherwise ideal BSCF crystals as the Frenkel pairs (in particular, oxygen defects, Table 1) have a lower energy than the energy required for formation of single isolated (or rather well-separated) vacancies in the lattice.

The original ideal supercells in our calculations were designed in such a way that the minimum anisotropy of the ionic distribution in the crystalline lattice is introduced. In other words, metals of the same chemical type are placed in the supercell as far from each other as possible to ensure the most uniform distribution of ions and the highest degree of the crystal isotropy. This tactic yields the BSCF model crystals (Fig. 1) with the 50-50-75-25% composition, which simulates the closest to the most efficient BSCF 50-50-80-20% configuration determined experimentally. This model is also supported by both experimental [12] and theoretical [13] findings that Sr dopants in relevant materials $LaMnO_3$ and $LaCoO_3$ are distributed periodically in the crystalline lattices. In exploring how important the highly ordered composition is, we simulated possible rearrangements in the A- and B-type cation sublattice. For example, exchanging one Ba with one Sr in the supercell causes clustering of Sr and Ba perovskite phases as illustrated in Fig. 3, referred hereafter as the clustering effect. In a sense, this is another manifestation of the self-segregation process in the cation sublattices.

Energies describing the disorder in cation sublattice are summarized in Table 2. We found that a perturbation caused by the redistributions in either the A or B cation sublattices of the ABO_3 perovskite lattice does not require a significant additional energy. From the energetic point of view, this implies that both A metals (Ba and Sr) and B metals (Co and Fe) can be randomly distributed in the respective sites. The conclusion was additionally confirmed by the very low energies of less than 0.1 eV obtained for decomposition reactions (1) and (2) described in Table 3 (see more details below). Equation (1) may be interpreted as a complete separation of $Ba_xSr_{1-x}Co_{0.75}Fe_{0.25}O_3$ (x=0.5) into $BaCo_{0.75}Fe_{0.25}O_3$ and $SrCo_{0.75}Fe_{0.25}O_3$ (x=1,0). In the same way, equation (2) describes a full partition of $Ba_{0.5}Sr_{0.5}Co_{1-y}Fe_yO_3$ (y=0.25) into hexagonal $Ba_{0.5}Sr_{0.5}CoO_3$ cobaltite and cubic $Ba_{0.5}Sr_{0.5}FeO_3$ ferrate (y=0,1) perovskite phases.

Further, we predict that antisite substitutions, or a pair of defects in which an A metal occupies a B position of the ABO_3 lattice and the corresponding B metal fills the A position, (for example, Sr↔Co) are also possible. However, as expected, they require a significantly higher energy than the clustering of cations within the same sublattice due to the need for the charge compensation, the difference in ionic radii of A and B atoms, and the different coordination numbers in the ideal crystalline lattice. Table 2 demonstrates that a single A↔B cation exchange in a large 320 atom model supercell (64 BSCF formula units) requires 3.79-7.87 eV. This energy corresponds to a small concentration of such defects and turns out to be comparable to the vacancy formation energies.

Furthermore, we simulated a range of decomposition mechanisms of BSCF into other relevant perovskites and oxides (Table 3). Negative energy corresponds to an exothermic

reaction. Equation (1) represents the BSCF decomposition into Ba-rich $BaCo_{0.75}Fe_{0.25}O_3$ and Sr-rich $SrCo_{0.75}Fe_{0.25}O_3$ phases, while equation (2) describes the separation into Co-rich $Ba_{0.5}Sr_{0.5}CoO_3$ and Fe-rich $Ba_{0.5}Sr_{0.5}FeO_3$ phases. The obtained low energies confirm that significant solubility of metals within the corresponding sublattices may take place. The comparable total energies of BSCF and of the relevant limiting cases, corresponding to a combination of Ba/Sr and Co/Fe rich compositions suggest that BSCF likely to consist of several co-existing solid perovskite phases under ambient conditions.

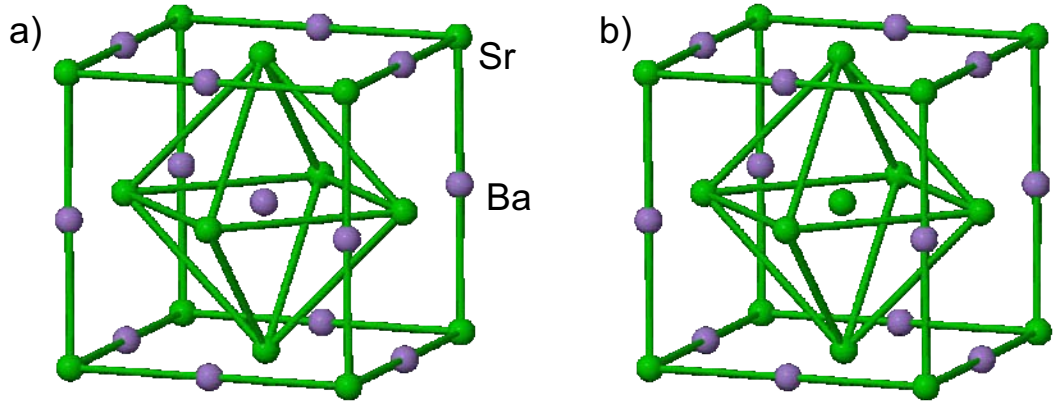

Figure 3. The clustering effect is illustrated with the Sr↔Ba exchange in the $Ba_{0.5}Sr_{0.5}Co_{0.75}Fe_{0.25}O_3$ crystal structure. In the original ideal supercell (a), the central A site is occupied by Ba while in the shown "defective" supercell (b), the site is occupied by Sr. For simplicity, only the A-cation sublattice of the ABO_3 perovskite structure is shown.

Table 1. Frenkel disorder in the $Ba_{0.5}Sr_{0.5}Co_{0.75}Fe_{0.25}O_3$ lattice. Standard Kröger and Vink notations for defects are used. The defect formation energy is calculated per one supercell containing eight BSCF formula units (40 atoms). Both the nearest defects (close pair) and the well-separated defects (distant pair) were modeled. The two possible oxygen vacancy configurations, were probed, the vacancy placed in between two Co atoms, $V_{Co\text{-}O\text{-}Co}$, and the vacancy placed in between Co and Fe atoms, $V_{Co\text{-}O\text{-}Fe}$. Both the split and channel configurations were probed for interstitials. In the split interstitial defect, a displaced atom forms a dumbbell with a regular atom in such a way that neither atom is on the ideal crystalline site but the two are symmetrically displaced from it. In the channel interstitial configuration, the displaced atom is located in the nearest hollow position.

Reaction	Energy per defect (eV)		Interstitial Configuration
	Close Pair	Distant Pair	
$Ba^{x}_{Ba} \leftrightarrow V''_{Ba}+Ba_i^{\cdot\cdot}$	4.89	6.00	Split
$Sr^{x}_{Sr} \leftrightarrow V''_{Sr}+Sr_i^{\cdot\cdot}$	5.40	4.94	Split
$Co^{y}_{Co} \leftrightarrow V'''_{Co}+Co_i^{\cdot\cdot\cdot}$	1.94	2.41	Channel
$Fe^{1-y}_{Fe} \leftrightarrow V''''_{Fe}+Fe_i^{\cdot\cdot\cdot\cdot}$	2.72	2.94	Channel
$O^{z}_{O} \leftrightarrow V^{\cdot\cdot}_{Co\text{-}\mathbf{O}\text{-}Co}+O_i''$	1.46	1.33	Split
$O^{z}_{O} \leftrightarrow V^{\cdot\cdot}_{Co\text{-}\mathbf{O}\text{-}Fe}+O_i''$	1.27	1.20	Split

Table 2. Energies of cation structural disorder in the BSCF lattice. Calculations are performed for a single exchange pair of cations placed in a large 320 atom model supercell, which consists of 64 BSCF formula units. Reactions (1) and (6) represent the clustering effect in A- and B- sublattices, respectively, and reactions (2)-(5) describe the formation of antisite defects.

N	Cation Exchange	Energy (eV)
1	Ba ↔ Sr	-0.20
2	Ba ↔ Co	6.16
3	Ba ↔ Fe	7.87
4	Sr ↔ Co	3.79
5	Sr ↔ Fe	5.70
6	Co ↔ Fe	0.08

Table 3. Stability of $Ba_xSr_{1-x}Co_yFe_{1-y}O_{3-\delta}$ with respect to decomposition reactions. All reactions are written for a specific set of *x, y,* and δ (x=0.5, y=0.75, and δ=0).

N	Reaction	Energy (eV)
1	$4BSCF \leftrightarrow 2BaCo_{0.75}Fe_{0.25}O_3 + 2SrCo_{0.75}Fe_{0.25}O_3$	-0.04
2	$4BSCF \leftrightarrow 3Ba_{0.5}Sr_{0.5}CoO_3 + Ba_{0.5}Sr_{0.5}FeO_3$	0.09
3	$4BSCF \rightarrow 2BaCoO_3 + SrCoO_3 + SrFeO_3$	-0.70
4	$4BSCF \rightarrow BaCoO_3 + 2SrCoO_3 + BaFeO_3$	-0.11
5	$4BSCF \rightarrow BaCoO_3 + SrCoO_3 + Ba_{0.5}Sr_{0.5}CoO_3 + Ba_{0.5}Sr_{0.5}FeO_3$	-0.37
6	$4BSCF \leftrightarrow BaO_2 + Co_2O_3 + BaCoO_3 + SrO + SrFeO_3$	-0.06
7	$4BSCF \rightarrow BaO_2 + SrO + Co_2O_3 + Ba_{0.5}Sr_{0.5}CoO_3 + Ba_{0.5}Sr_{0.5}FeO_3$	0.27
8	$4BSCF \rightarrow 2BaO_2 + Co_3O_4 + SrO + SrFeO_3$	2.11
9	$4BSCF \rightarrow BaO_2 + 2SrO + BaFeO_3 + Co_2O_3 + CoO + 1/2O_2$	3.34
10	$4BSCF \rightarrow BaCoO_3 + 2SrO + BaO_2 + 2/3Co_3O_4 + 1/3Fe_3O_4 + 1/2O_2$	3.77
11	$4BSCF \rightarrow 2BaO_2 + 2CoO + SrCoO_3 + SrFeO_3$	4.06
12	$4BSCF \rightarrow BaO + 2SrO + BaFeO_3 + Co_3O_4 + O_2$	5.28
13	$4BSCF \rightarrow 2BaO_2 + 2SrO + Co_3O_4 + FeO + 1/2O_2$	5.57
14	$4BSCF \rightarrow 2BaCoO_3 + CoO + 2SrO + FeO + O_2$	5.56
15	$4BSCF \rightarrow BaCoO_3 + SrCoO_3 + SrO + BaO + 1/2Co_2O_3 + 1/2Fe_2O_3$	6.49
16	$4BSCF \rightarrow BaO + BaCoO_3 + Co_2O_3 + 2SrO + FeO$	12.33
17	$4BSCF \rightarrow BaO + SrO + 2CoO + Ba_{0.5}Sr_{0.5}CoO_3 + Ba_{0.5}Sr_{0.5}FeO_3 + O_2$	13.74

We also established that decomposition into the two-component parent perovskites (ABO_3), such as $BaCoO_3$, $SrCoO_3$, and (Sr/Ba)FeO_3 proceeds in accordance with weakly exothermic reactions (see equations (3) and (4) in Table 3). $BaCoO_3$ has a lower energy in the hexagonal phase than in a cubic phase. $BaFeO_3$ also happened to favor the

hexagonal phase over the cubic arrangement. Equation (5) demonstrates another, also slightly exothermic possibility of decomposition into a mixture of four perovskites. These conclusions are in agreement with the XRD experiments and TEM analysis, which demonstrated that at a temperature of 1073 K in air, the equilibrium phases are hexagonal and cubic perovskites [6].

On the other hand, most reactions that describe the decomposition with involvement of binary oxides are endothermic, require a higher energy, and are considered lower probability processes. The only exception is equation (6), which unexpectedly turned out to be exothermic. This result is somewhat counterintuitive as a high cohesive energy of a perovskite crystalline lattice should prevent the decomposition into simple oxides as exemplified by a fairly high energy of equation (13). We predict that the presence of oxygen vacancies in the lattice may facilitate some of the indicated decomposition routes. For example, reactions (9-10), (12-14) and (17) contain oxygen in the gas state among the reaction products, which implies that the left side of the equation that represents the original BSCF crystal, likely to have some concentration of oxygen vacancies. Further study of energetic aspects of this possibility in the nonstoichiometric BSCF is of great interest.

Summary and Conclusions

Point defects and the lattice stability were explored by means of *ab initio* DFT calculations performed by using large supercells and variety of ideal and defective BSCF related crystalline structures. We established that the complexity of the BSCF crystalline arrangement leads to a possibility to accommodate many variations of point defects in the lattice and determines its chemical stability. Cation clustering of A or B type of metals requires a low energy, implying that the distribution of metals in the BSCF lattice is not necessarily highly ordered while the formation of antisite defects is much more energetically costly. Frenkel disorder is preferred over Schottky disorder. More importantly, based on thermodynamic considerations, BSCF is expected to be composed of an equilibrium mixture of several perovskite phases and there are several alternative routes that lead to its decomposition into a combination of cubic and hexagonal perovskites. More accurate analysis (in progress) will take into account entropy effects at real temperatures and kinetics of the cation diffusion processes. The obtained results are consistent with available experimental observations and allow for reliable predictions of the BSCF behavior under a range of conditions. This research is imperative for exploring the potential use of complex perovskites as SOFC cathodes and gas separation ceramic membranes. The obtained results will help to develop recommendations for synthetic chemists and chemical engineers regarding the enhancement of BSCF's (and other materials') function of converting energy by optimizing their chemical composition.

Acknowledgements

This research was supported in part by the EC FP7 NASA-OTM project, DoE Contract DE-AC02-05CH11231 (NERSC resources) and National Science Foundation (NSF). Any appearance of findings, conclusions, or recommendations, expressed in this material are those of the authors and do not necessarily reflect the views of NSF. This

References

1. L.Wang, R. Merkle, J. Maier, *J. Electrochem. Soc*., **157**, B1802 (2010).
2. W. Zhou, R.Ran and Z.Shao, *J. Power Sources*, **192**, 231 (2009).
3. L.Wang, R. Merkle, J. Maier, *ECS Trans.*, **25**, 2497 (2009).
4. Yu. Mastrikov, M.M. Kuklja, E.A. Kotomin, J. Maier, *En. Env. Sci*., **3,** 1544 (2010).
5. E.A. Kotomin, Yu. Mastrikov, M.M. Kuklja, R. Merkle, A. Roytburd, J.Maier, *Solid State Ionics*, 2010, DOI: 10.1016/j.ssi.2010.10.011.
6. D. Mueller, R. A. De Souza, T. E. Weirich, D. Roehrens, J. Mayer and M. Martin, *Phys. Chem. Chem. Phys.,* **12**, 10320 (2010).
7. S. Yakovlev, C.-Y. Yoo, S. Fang, H.J.M. Bouwmeester, *Appl. Phys. Lett*., **96**, 254101 (2010).
8. G. Kresse, J. Furthmueller, VASP the Guide: Univ. Vienna, 2003.
9. H. J. Monkhorst, J. D. Pack, *Phys. Rev. B,* **13**, 5188 (1976).
10. G. Henkelman, A. Arnaldsson, and H. Jónsson, *Comp. Mater. Sci.*, **36**, 254 (2006).
11. B. S. Thomas, N. A. Marks, B. D. Begg, *Nucl. Inst. Meth. B*, **254**, 211 (2007).
12. Z.L. Wang, J. Zhang. Phys. Rev. B 54, 1153 (1996).
13. D. Fuks, L. Bakaleinikov, E.A. Kotomin et al., *Solid State Ionics*, **177**, 217 (2006).